Cerebral Cortex, 2017; 1–14

doi: 10.1093/cercor/bhx251
Original Article

ORIGINAL ARTICLE

The Bat as a New Model of Cortical Development

Verónica Martínez-Cerdeño[1,2,7], Jasmin Camacho[1,2], Jeanelle Ariza[1,2], Hailee Rogers[1,2], Kayla Horton-Sparks[1,2], Anna Kreutz[3], Richard Behringer[4], John J. RasweilerIV[5] and Stephen C. Noctor[6,7]

[1]Department of Pathology and Laboratory Medicine, UC Davis School of Medicine, Sacramento, CA, USA, [2]Institute for Pediatric Regenerative Medicine and Shriners Hospitals for Children Northern California, Sacramento, CA, USA, [3]Neuroscience Graduate Program, UC Davis, Davis, CA, USA, [4]Department of Genetics, University of Texas MD Anderson Cancer Center, Houston, TX, USA, [5]Department of Obstetrics and Gynecology, State University of New York Downstate Medical Center, Brooklyn, NY, USA, [6]Department of Psychiatry and Behavioral Sciences, UC Davis School of Medicine, Sacramento, CA, USA and [7]MIND Institute, UC Davis School of Medicine, Sacramento, CA, USA

Address correspondence to: Stephen C. Noctor, UC Davis MIND Institute, 2805 50th street, Sacramento, CA 95817, USA. Email: scnoctor@ucdavis.edu; Verónica Martínez-Cerdeño, Shriners Hospital 2425 Stockton BLVD, Sacramento CA 95817, USA. Email: vmartinezcerdeno@ucdavis.edu

Abstract

The organization of the mammalian cerebral cortex shares fundamental features across species. However, while the radial thickness of grey matter varies within one order of magnitude, the tangential spread of the cortical sheet varies by orders of magnitude across species. A broader sample of model species may provide additional clues for understanding mechanisms that drive cortical expansion. Here, we introduce the bat *Carollia perspicillata* as a new model species. The brain of *C. perspicillata* is similar in size to that of mouse but has a cortical neurogenic period at least 5 times longer than mouse, and nearly as long as that of the rhesus macaque, whose brain is 100 times larger. We describe the development of laminar and regional structures, neural precursor cell identity and distribution, immune cell distribution, and a novel population of Tbr2+ cells in the caudal ganglionic eminence of the developing neocortex of *C. perspicillata*. Our data indicate that unique mechanisms guide bat cortical development, particularly concerning cell cycle length. The bat model provides new perspective on the evolution of developmental programs that regulate neurogenesis in mammalian cerebral cortex, and offers insight into mechanisms that contribute to tangential expansion and gyri formation in the cerebral cortex.

Key words: bat, cortical development, neurogenesis, subventricular zone, ventricular zone

Introduction

The organization of the mammalian cerebral cortex shares fundamental features across species in both the radial and tangential dimensions. In the radial dimension the cerebral cortex is organized into discrete layers, with each layer composed of distinct cell types that exhibit characteristic morphology, connectivity, and function. In the tangential dimension, the cortical sheet is organized into discrete areas that receive information from distinct sensory modalities and brain regions, and perform specific functions. While the thickness of the cortical gray matter varies across species, those differences are within an order of magnitude. In contrast, differences in the surface area or tangential spread of the cortical sheet vary greatly.

Alterations in cell production and/or daughter cell survival can affect the final number of cells that populate the cortical gray matter, and thereby impact the radial and/or tangential surface area of the cortex. Among parameters of cell production, an increased number of precursor cells, an extended

period of cell production, or a shortened cell cycle could each increase cell production and potentially increase the size of the cortical sheet. Nonetheless, the mechanisms that regulate the size of the cortical sheet are not yet well understood. A variety of mammalian species have been used to study the dynamics of cell production in the developing cerebral cortex, particularly mice and rats within the order Rodentia. While studies in Carnivora (e.g., ferret) and more recent studies in primates such as macaque and human have provided important new details, studying species from other mammalian orders may provide additional clues for understanding the mechanisms that drive development and evolution of the mammalian cortex.

Most cortical cells are produced by precursor cells that reside in proliferative zones that surround the telencephalic ventricles: the ventricular zone (VZ) directly adjacent to the ventricle and the subventricular zone (SVZ) superficial to the VZ. Work in human, macaque monkeys, and other gyrencephalic mammals has shown that the SVZ is subdivided into distinct proliferative zones: an inner SVZ (iSVZ) and outer SVZ (oSVZ) (Smart et al. 2002; Fietz et al. 2010; Hansen et al. 2010; Reillo et al. 2011; Martinez-Cerdeno et al. 2012). The oSVZ is also present in the rat during late gestation (Martinez-Cerdeno et al. 2012). Work in many mammalian species has identified primary precursor cells called radial glial (RG) cells that reside in the VZ. Radial glia can be positively identified based on the expression of the transcription factor Pax6 (Gotz et al. 1998), interkinetic nuclear movements during the cell cycle with division at the surface of the ventricle (Sauer 1935; Seymour and Berry 1975; Takahashi et al. 1993; Noctor et al. 2001, 2008; Miyata et al. 2004), and characteristic bipolar morphology featuring a long thin pial process. Secondary precursor cells that populate the SVZ have also been well characterized. These cells, which we call intermediate progenitor cells (Martinez-Cerdeno and Noctor 2016), can be identified based on Tbr2 expression (Englund et al. 2005), lack of interkinetic nuclear movements during mitosis, cell division that most often occurs away from the ventricle, and a multipolar morphology (Noctor et al. 2004, 2008).

An additional precursor cell type that has been identified in mammalian cortex is the translocating RG cell (Noctor et al. 2004, 2008), or oRG cell (Hansen et al. 2010). These cells express astroglial cell markers and have been identified in nonhuman primate (Schmechel and Rakic 1979), ferret (Voigt 1989), human (deAzevedo et al. 2003), and rat (Noctor et al. 2004). The translocating RG cells detach from the ventricle, migrate through the SVZ, and in the rat undergo divisions that generate non-neuronal daughter cells (Noctor et al. 2008). Later work showed that across a broad array of mammalian species translocating RG cells located in the SVZ express Pax6, but not Tbr2 (Fietz et al. 2010; Hansen et al. 2010; Reillo et al. 2011; Martinez-Cerdeno et al. 2012).

Radial glia and intermediate progenitor cells have been identified in the developing cerebral cortex of all mammals investigated to date and other vertebrates including reptiles and birds (Martinez-Cerdeno et al. 2016). The number of species in which translocating RG cells are present in the developing cerebral cortex is under study. Differences in the number and distribution of these precursor cells across species suggest they play a role in the developmental and evolutionary expansion of the cortical sheet. Yet, factors that regulate the growth of mammalian cortex, particularly in the tangential dimension, are not well understood. Based on our previous studies of cortical development in nonmammalian species (reptiles, birds), mammalian species with lissencephalic cortex (rodents), and mammalian species with gyrencephalic cortex (ferret, macaque, human), we hypothesized that the evolution of a 2-step pattern of cell division played an important role in the expansion of the cerebral cortex (Martínez-Cerdeño et al. 2006). In this scheme, precursor cells divide first in the VZ, and later undergo amplifying divisions in the SVZ in a manner that amplifies neuron production.

We present here, for the first time, the bat brain as a tool for studying cortical development. Bats have unique features among mammals, an incredible taxonomic diversity, and represent at least 20% of all mammalian species (Graham and Reid 2001). Bats had initially been proposed as closely related to shrews and perhaps "flying lemurs", but recent molecular analyses have placed bats (Order Chiroptera) within the superorder *Laurasiatheria* that includes carnivores and ungulates (Nery et al. 2012). Bats were initially divided into the suborders megachiroptera and microchiroptera based primarily on characteristics such as body size and use of echolocation. Those assigned to megachiroptera were larger, weighing an average of 200 g with some weighing up to 1.6 kg. Bats assigned to microchiroptera were much smaller, often weighing <30 g, and were associated with the use of echolocation. However, ongoing studies based on genetics, rather than behavioral or morphological characteristics, propose the placement of individual bat species within the suborders Yinpterochiroptera and Yangochiroptera, with species using echolocation found in both suborders (Springer 2013).

The size of bats varies among the hundreds of species. Correspondingly, the size of the adult bat brain recorded in some studies varies from approximately 0.7–2.6 g (Baron et al. 1996), with brain weights even lower among some of the smaller species. The adult "microbat" brain ranges in size from that of an adult mouse (~0.4 g) to that of a rat (~2 g). The length of gestation among bats varies from 40 days to 6 months. Despite the large number of bat species (>1300) distributed around the world, little is known about their brain development, in particular how it compares or contrasts to that in other mammals. Here we describe for the first time the development of the cerebral cortex of a bat species, the short-tailed fruit bat (*Carollia perspicillata*). *Carollia perspicillata* may be the most common mammal inhabiting the lowland tropics of the New World. It is also the only bat in which timed pregnancies can be readily generated and followed in animals maintained in a controlled laboratory setting (Rasweiler et al. 2009).

We show here that the neurogenic stage of cerebral cortex development in the bat *C. perspicillata* extends for a period of nearly 50 days. Although the brain of *C. perspicillata* is similar in size to that of a mouse, the cortical neurogenic period is at least 5 times longer than that of the mouse and nearly as long as that of the rhesus macaque, whose brain is over 100 times larger. These data suggest that unique mechanisms guide cortical development in the bat, particularly concerning length of the cell cycle. We propose that the bat model may yield new perspective on the evolution of developmental programs that guide formation of mammalian cerebral cortex. These studies will provide new insight into mechanisms that contribute to tangential expansion of the cerebral cortex and formation of cortical gyri in mammals.

Materials and Methods

Animals

Bats were collected from the wild in Trinidad as described previously (Cretekos et al. 2005; Rasweiler et al. 2009). Wild-caught

specimens were collected, processed and exported with the permission of the Wildlife Section, Forestry Division of the Ministry of Agriculture, Land and Fisheries of the Republic of Trinidad and Tobago. *Carollia perspicillata* were collected from a reproductively synchronized, wild population living on the island of Trinidad during the month of May. Each specimen was staged using a system based upon limb development in embryos collected from carefully timed pregnancies in captive-bred animals (Cretekos et al. 2005).

Although *C. perspicillata* is capable of taking pregnancies into substantial delays, the embryos incorporated in this study were assumed to have been developing at a normal rate. All had progressed beyond the primitive streak stage, at which pregnancies in this species are sometimes subject to delay, and no evidence of embryonic delays has been observed in *C. perspicillata* collected during May on Trinidad.

Adult females in the Trinidadian population generally exhibit two pregnancies per year. The first appears to commence in most adult females in October or possibly earlier and includes a significant period of delay at the primitive streak stage. This lengthens gestation by an estimated minimum of 44–50 days, although the delay could be longer. Soon after parturition (which most frequently occurs in March or April), these females experience a post-partum estrus and become pregnant again. Extensive sampling, conducted annually from 2000 to 2015, indicates that this second pregnancy does not include a significant period of embryonic delay (Rasweiler and Badwaik 1997; Badwaik and Rasweiler 2001; Rasweiler JJ IV, RR Behringer & CJ Cretekos, unpublished observations).

Pregnant females were euthanized by cervical dislocation between 2 and 4 h after collection. Fetuses, one per female, were extracted and perfused intracardially with PBS followed by 4% paraformaldehyde in PBS (PFA). Fetal brains were removed and stored in PFA for 24 h post fixation.

Tissue Staining

Nissl

Sections were stained with cresyl violet (Sigma) at 37 °C for 1–10 min, dehydrated with graded alcohols, differentiated with glacial acetic acid, treated with xylene, and coverslipped with DPX (Fluka). Nissl-stained tissue was imaged on a Zeiss microscope equipped with an Axiocam camera (Zeiss). Statistical analysis was performed using Instat (GraphPad Software). The number of mitotic precursor cells in prenatal bat cortex was quantified in Nissl-stained tissue. The number of mitoses in the developing bat cortex was quantified in 70 μm wide bins that extended radially from the ventricle to the pial meninges. Bins were positioned in the dorsal cortex of coronal sections at the level of the midline crossing of the anterior commissure. The number of mitoses in the bins was counted at the ventricular surface and away from the ventricle—in abventricular positions. Results were graphed and compared to data gathered from rat and ferret cortical tissue using the same quantification method (Martínez-Cerdeño et al. 2006).

Immunostaining

Brains were sectioned at 14 μm coronal slices prepared on a cryostat (Leica) and mounted on glass slides (Fisher). Sections were blocked in 10% donkey serum (Gibco), 0.1% Triton X-100 and 0.2% gelatin (Sigma). Sections were incubated for 24 h at room temperature with the following primary antibodies: 4A4 (mouse monoclonal 1:1000, MBL), Tbr2 (chicken polyclonal 1:200, Millipore), Pax6 (rabbit polyclonal 1:200, Biolegend), and Iba1 (1:500, Dako). Sections were rinsed with PBS and incubated for 1 h in with secondary antibodies conjugated with Cy2, Cy3, or Cy5 conjugated polyclonal anti-mouse/goat/rabbit antibodies (1:100, Jackson Lab). Antibodies were diluted in incubation buffer containing 2% normal donkey serum, 0.02% Triton X-100 and 0.04% gelatin. Sections were then rinsed in PBS and incubated with DAPI 1:1000 (Roche) for 15 min to label nuclei. We omitted the first antibody as a control for each immunostaining experiment. All imaging was performed on an Olympus Fluoview confocal laser microscope and analysis performed in Fluoview v.3.3 (Olympus).

Results

We analyzed brains from adult and developmental stages of short-tailed fruit bats, *C. perspicillata* (Fig. 1A), collected from the island of Trinidad, West Indies. We collected embryos at different stages of prenatal development and assigned a Carnegie

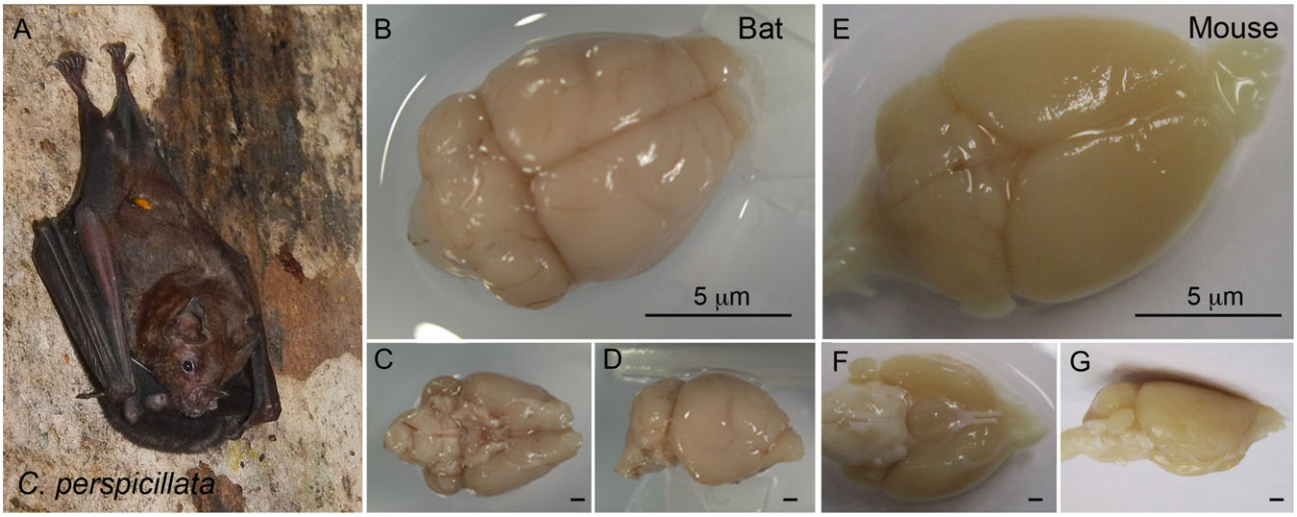

Figure 1. (*A*) Adult *C. perspicillata* with a baby under the wings. (*B–D*) Dorsal, ventral and lateral views of the adult *C. perspicillata* brain. (*E–G*) Dorsal, ventral, and lateral views of adult mouse brain are shown for comparison. Scale bar: 1 mm.

Stage and an estimated embryonic day of gestation based on standard morphological features, as limb development, as described for carefully timed pregnancies in captive-bred animals (Cretekos et al. 2005). Brains were frozen, cut, one slice series stained for Nissl and additional series immunostained. Our initial goal was to map out the neurogenic period of cerebral cortex development in *C. perspicillata*. Since these studies did not include the use of birthdating agents we relied on cytoarchitectural analyses to identify the stages of proliferative zone development and cortical plate formation that correspond to cortical neurogenic stages in well-studied mammalian species. The current analysis focuses on the dorsal cortex.

Examination of gross brain structures demonstrated that the cerebral cortex of the adult *C. perspicillata* is mostly lissencephalic (Fig. 1), like the mouse brain, but with subtle sulci apparent on the lateral surface of the cerebrum. The weight of the adult brain in *C. perspicillata* averaged 0.588 g ($n = 3$), similar to that of adult mice (0.4 g), but less than that of adult rats at ~2 g.

Development of Laminar and Regional Structures in *C. perspicillata*

The sequence of *C. perspicillata* cerebral cortex development is similar to that of mouse, but with important distinctions. The anterior pole of the neural tube in *C. perspicillata* closes at CS11, prior to embryonic day (E)40 of gestation. At this stage the forebrain consists primarily of the proliferative VZ and a thin meningeal layer. Between CS12 and CS15, corresponding to E40 and E46, the thickness of the VZ did not increase significantly in the radial dimension, but expanded tangentially. As a result, the telencephalic vesicle and the size of the telencephalon increased. Until CS15 the medial and lateral ganglionic eminences (MGE/LGE) were discernable as distinct structures, as in the E15 rat (Altman and Bayer 1995). At CS15 the VZ was 60 to 80 μm thick and consisted of radially oriented cells (Fig. 2A).

At CS16, which corresponds to gestation day E50, the cortical plate was not yet visible. The telencephalon consisted of the proliferative VZ and the marginal zone. At CS16 the MGE and LGE had fused into a single ganglionic eminence, as occurs by approximately E17 in the rat (Altman and Bayer 1995). The VZ was 80–120 μm thick (Fig. 2B).

By CS17 (gestation day E54) the SVZ had become apparent and the cortical plate was present in lateral cortex but did not yet extend fully to medial cortex. The VZ was approximately 100 μm thick, and the VZ and SVZ together measured approximately 130 μm (Fig. 2C). The lack of a cortical plate at CS16 (E50), and appearance of the cortical plate 4 days later by CS17 suggested that neurogenesis of deep layer neurons began around CS16. The sequence of cortical plate emergence in bat during the period from CS16 to CS17 matches that in rat during the period from E15 to E17, when peak layer 6 neurogenesis begins and the cortical plate forms in lateral cortex (Bayer and Altman 1991). These data indicate that bat cerebral cortex follows the same lateral to medial gradient of neurogenesis and cortical plate formation that has been described in rat (Bayer and Altman 1991), and are consistent with the concept that cortical neurogenesis begins by CS16 in *C. perspicillata*.

At CS18 (E60) the cortical plate extended to the medial wall of the telencephalon and had grown thicker in the radial dimension, appearing to consist of neurons destined for layers 5 and 6. The VZ ranged from 80 to 100 μm thick along the rostro-caudal axis, and the VZ and SVZ together measured 100–120 μm in thickness. At subsequent stages the VZ became appreciably thinner, the SVZ became slightly thicker, and the cortical plate grew in the radial dimension as cortical neurons for more superficial layers migrated into position (Figs 2D and 3). Our analysis of the proliferative zones suggests that during CS19 (E64) layer 5 neurons were added to the cortical plate; at CS20 (E70) layers 5 and 4; at CS21 (E75) layer 4; at CS22 (E80) layer 3 neurons; at CS23 (E85) primarily layer 2; and that CS24 (E90) represented the end of layer 2 formation as the cortical plate appeared to be fully formed (Fig. 4).

Neural Precursor Cell Distribution Across Development in *C. perspicillata*

We quantified the number and distribution of precursor cells that were undergoing division at the ventricular surface and away from the ventricle at stages of development encompassing the onset and completion of neurogenesis in the dorsal bat neocortex. Sections of Nissl-stained tissue were photographed and the number and location of mitotic figures in the dorsal cortex were recorded in 70 μm wide bins that extended from the ventricular surface to the pia. Bin size was chosen for comparison with data gathered previously from other species (Martínez-Cerdeño et al. 2006). Images of Nissl-stained tissue used for analysis are shown in Figure 5.

Qualitative analysis showed that from CS11 through CS15 mitotic precursor cells throughout the cortex divided exclusively at the ventricular surface. At CS16 there were numerous mitoses at the ventricular surface, but we did not observe abventricular divisions in the dorsal cortex (Fig. 5B). However, abventricular divisions were present in the ganglionic eminence of the CS16 bat. CS17 was the stage when peak cell division occurred at the ventricular surface of dorsal cortex. It was also the stage when abventricular mitoses first appeared in the dorsal cortex (Fig. 5C). Abventricular mitoses were present in the VZ, the SVZ and intermediate zone as in other species (Noctor et al. 2008; Martinez-Cerdeno et al. 2012), but the majority of divisions was located in the SVZ just superficial to the VZ, as in mouse (Smart 1973). Through CS20 (E70) the majority of divisions occurred at the surface of the ventricle while the number of abventricular mitoses remained relatively low (Fig. 5D).

At CS22 the number of ventricular surface mitoses dropped substantially and the VZ shrank to a thin layer that was only 2 or 3 cells thick (Fig. 5E). In contrast, the size of the SVZ expanded and the majority of precursor cell divisions shifted to the SVZ. A similar shift in the location of precursor cell divisions from the ventricular surface to the SVZ occurs in many mammals including rat (Hamilton 1901; Martínez-Cerdeño et al. 2006; Martinez-Cerdeno et al. 2012), mouse (Smart 1973), ferret (Martínez-Cerdeño et al. 2006; Martinez-Cerdeno et al. 2012), and monkey (Smart et al. 2002; Martinez-Cerdeno et al. 2012). At CS22 the SVZ was most robust in the rostral cortex where numerous abventricular divisions occur. Whether this represents production of cells for both dorsal cortex and the rostral migratory stream remains to be determined for the bat.

By CS24 the number of ventricular mitoses had decreased substantially. The number of abventricular mitoses also decreased, but dividing precursor cells were present in the SVZ (Fig. 5F). Figure 6 shows the relative number of mitoses at the surface of the ventricle and in abventricular positions—including the SVZ—from CS16 to CS24.

We next compared the number of precursor cell divisions within radial bins of the bat VZ and SVZ to data we gathered from other mammals. The peak number of mitoses per unit length of ventricle surface was much lower in bat than in rat or ferret. As in all other mammals studied to date, the bulk of

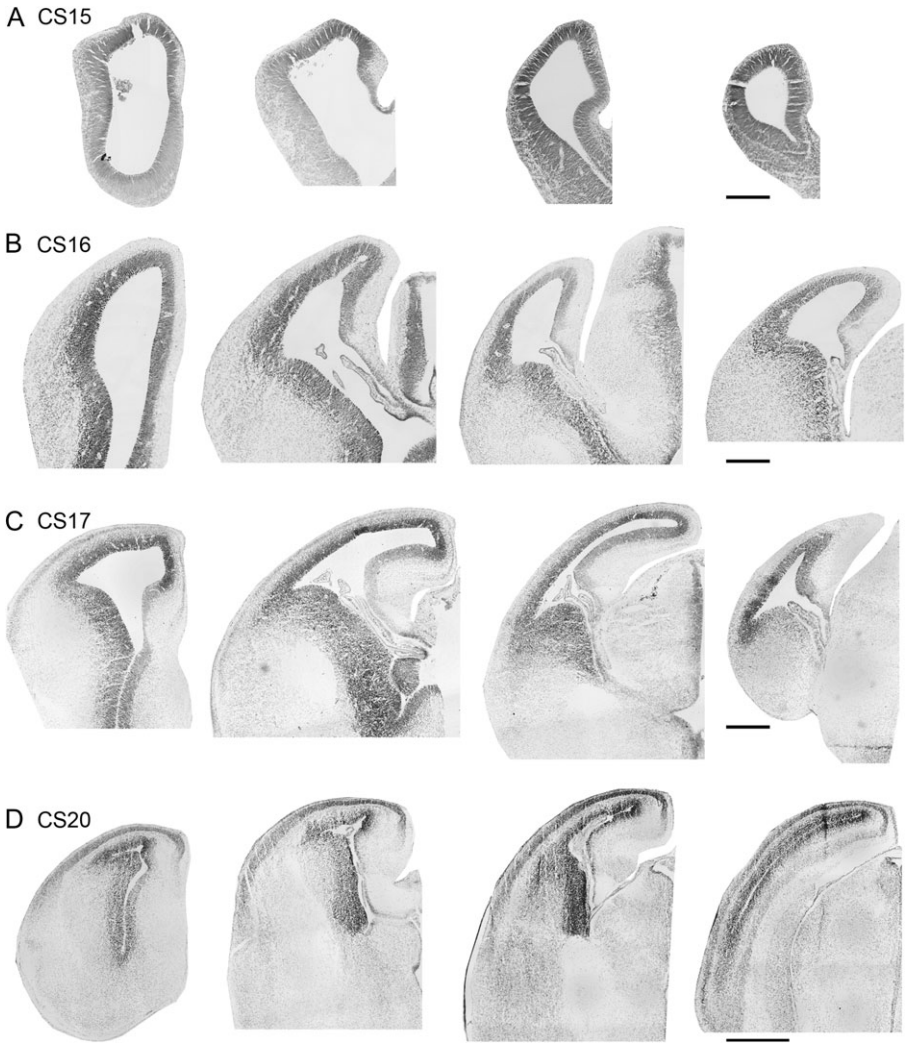

Figure 2. Sections of Nissl-stained tissue from prenatal bat brain. Four representative coronal sections along the rostro-caudal axes are shown for CS15 (*A*), CS16 (*B*), CS17 (*C*), and CS20 (*D*). At CS15 and CS16, the cortex primarily consists of a dense VZ band surrounding the lateral ventricle and a thin marginal zone. The cortical plate (CP) became visible at CS17. Scale bars: 1 mm.

divisions in the developing bat neocortex shifted to the SVZ over the course of the neurogenic period. Nonetheless, the number of ventricular and abventricular divisions in bat neocortex was substantially lower than that in rat or ferret (Fig. 7).

Molecular Identity of Neural Precursor Cells in *C. perspicillata*

We next tested the identity of precursor cells in the embryonic bat VZ and SVZ. We labeled sections of neocortical tissue from each stage with cell-specific antibodies that label cortical precursor cells in other mammalian and vertebrate brains (Gotz et al. 1998; Englund et al. 2005; Hansen et al. 2010; Martinez-Cerdeno et al. 2012, 2016). We included phosphorylated vimentin (4A4) to label M-phase dividing precursor cells; Pax6 to label RG cells in the VZ and translocating RG cells in the SVZ; and Tbr2 to label IP cells (Fig. 8).

Pax6 immunostaining produced a band of labeled cells in the bat VZ similar to that in the developing rodent brain. Pax6 expression was noted in the VZ at each stage we examined (Fig. 8). Precursor cells undergoing division at the surface of the ventricle were Pax6+ as in rat, ferret, and monkey (Martinez-Cerdeno et al. 2012).

Tbr2 immunostaining also revealed similarities with previously studied vertebrates. In the bat dorsal cortex at CS15, we observed a small number of Tbr2+ cells in the superficial portion of the VZ (Fig. 8A), similar to that we have observed in the E12 rat (Noctor et al. 2008). The number of Tbr2+ cells in the dorsal cortex increased in subsequent stages. At CS16, CS17 and CS18 there was a prominent band of Tbr2+ cells superficial to the VZ, as occurs in the rat between E17 and E20 (Noctor et al. 2008). At CS16 through CS18 we also noted that Tbr2+ cells were dispersed throughout the VZ in dorsal cortex (Fig. 8B, C, D). Tbr2 immunopositive cells were present in the developing bat cortex through CS25. In the CS22 cortex, the VZ was reduced in thickness and contained a small number of Tbr2+ cells. Numerous Tbr2+ cells interspersed with Pax6+ cells were present in dense bands away from the ventricle in the rostral and caudal poles of the telencephalon (Figure 9). This pattern was similar to the distribution of Tbr2+ cells in the outer SVZ that we have observed in late gestation rat neocortex (Martinez-Cerdeno et al. 2012).

We tested if Tbr2+ cells in the bat neocortex were mitotic through 4A4/Tbr2 double immunostaining. We found that mitotic

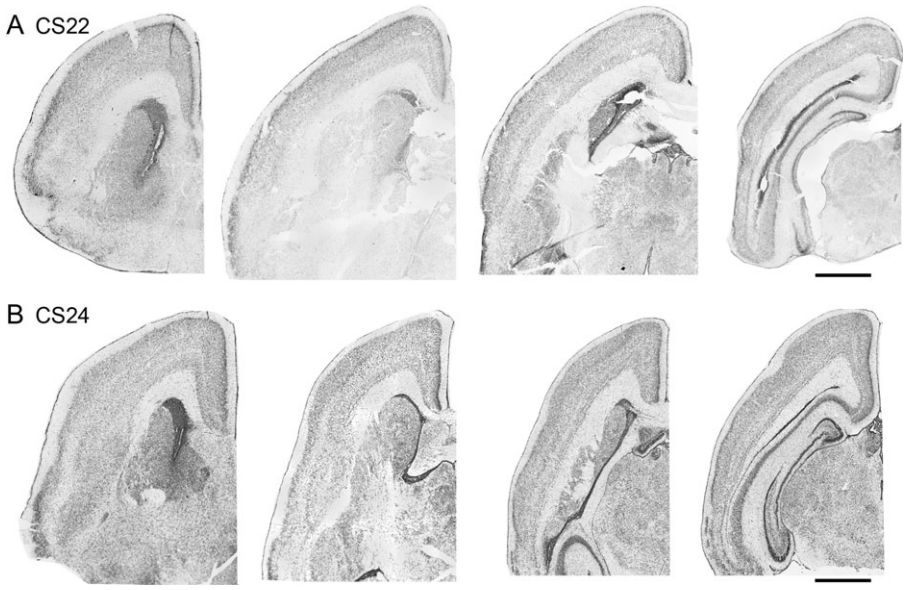

Figure 3. Sections of Nissl-stained tissue from prenatal bat brain. Four representative coronal sections along the rostro-caudal axes are shown for CS22 (*A*), and CS24 (*B*). At CS22 a dense proliferative zone is present around the lateral ventricle and the cortical plate was appreciably thicker. At CS24 the proliferative zones are thinner and the cortical layers more differentiated. Scale bars: 1 mm.

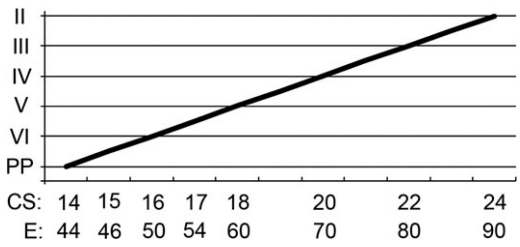

Figure 4. Timeline of cortical layer formation in *C. perspicillata*. Qualitative assessment of the VZ, SVZ, and cortical plate, transcription factor expression, and precursor cell mitoses in the cerebrum indicate the timeline of cortical layer genesis in *C. perspicillata*, beginning at CS14 (E44) and completing by CS23/CS24 (E85/90).

Tbr2+ cells were located in the SVZ, throughout the VZ, and at early stages of development were also located at the surface of the ventricle (Fig. 10C). Mitotic Tbr2+ cells were observed in the bat neocortex from CS16 through CS23 (Figs 9 and 10). These data further support the concept that cortical neurogenesis in *C. perspicillata* begins before CS16 (E50) and continues at least through CS23 (E85).

We found that Tbr2+ cells were present in both dorsal proliferative zones and the caudal ganglionic eminence (CGE) during early stages of cortical neurogenesis in bat. At CS16 and CS17 Tbr2+ cells were present in the dorsal neocortex, but were not expressed in the MGE or LGE. However, Tbr2+ cells were present in the SVZ of the well-defined CGE of the bat at CS16 and CS17 (Fig. 10A, B). For comparison, we immunostained coronal sections of E17 rat neocortex and found no Tbr2 expression in the CGE (data not shown). By CS18, and at all subsequent stages of bat cortical development, Tbr2+ cells were restricted to the dorsal proliferative zones.

Across the developmental stages we examined, some mitotic cells in the SVZ expressed only Pax6, while others expressed both Pax6 and Tbr2 (Figs 9 and 10). Based on previously published work in human (Fietz et al. 2010; Hansen et al. 2010), monkey (Martinez-Cerdeno et al. 2012), ferret (Fietz et al. 2010; Martinez-Cerdeno et al. 2012) and rat (Martinez-Cerdeno et al. 2012), we infer that the mitotic SVZ cells that express only Pax6 in the bat are translocating RG cells, while those that express both Pax6 and Tbr2 are likely IP cells that retain Pax6 protein from their mother RG cell. Consistent with this idea we observed 4A4+ precursor cells in the bat SVZ that exhibited the morphology of translocating RG cells and expressed Pax6 but not Tbr2 (Fig. 9C, yellow arrowheads).

Neuroimmune Cells in the Developing Cortex of *C. perspicillata*

We next immunostained cortical tissue from select stages of bat development with anti-Iba1 antibodies to examine colonization of the bat cerebral cortex with microglial cells. At the start of cortical neurogenesis in the CS16 bat (E50), the number of microglial cells in the bat cortex was very low. Iba1+ cells were present in the meninges, but very few Iba1+ cells were observed within the cortical parenchyma (Fig. 11A, C). At CS20 (E70) the number of microglial cells remained low (Fig. 11B). The distribution pattern of microglial cells in the CS16 and CS20 bat was similar to that we described in the E12 and E17 rat (Cunningham et al. 2013). At CS22 (E80) the distribution of microglial cells in the bat neocortex was very sparse in comparison to that seen in rat at a comparative stage of cortical neurogenesis (approximately E21). By CS24 (E90) the number of microglia had dramatically increased and microglial cells were distributed evenly across the cortical wall (Figure 11D), similar to that present in the postnatal week 2 rat (Cunningham et al. 2013).

At CS16, CS20, and CS22, microglial cells exhibited the striking morphology of "activated" cells that we have previously described in prenatal rat and monkey brain (Cunningham et al. 2013; Ibanez Rodriguez et al. 2016). In contrast to microglia in the healthy adult cerebral cortex that have a relatively small soma and multiple finely branched processes, microglia in the prenatal bat brain often had an enlarged ameboid soma with a small number of thick processes (Fig. 11E, F, I, and J). By CS24

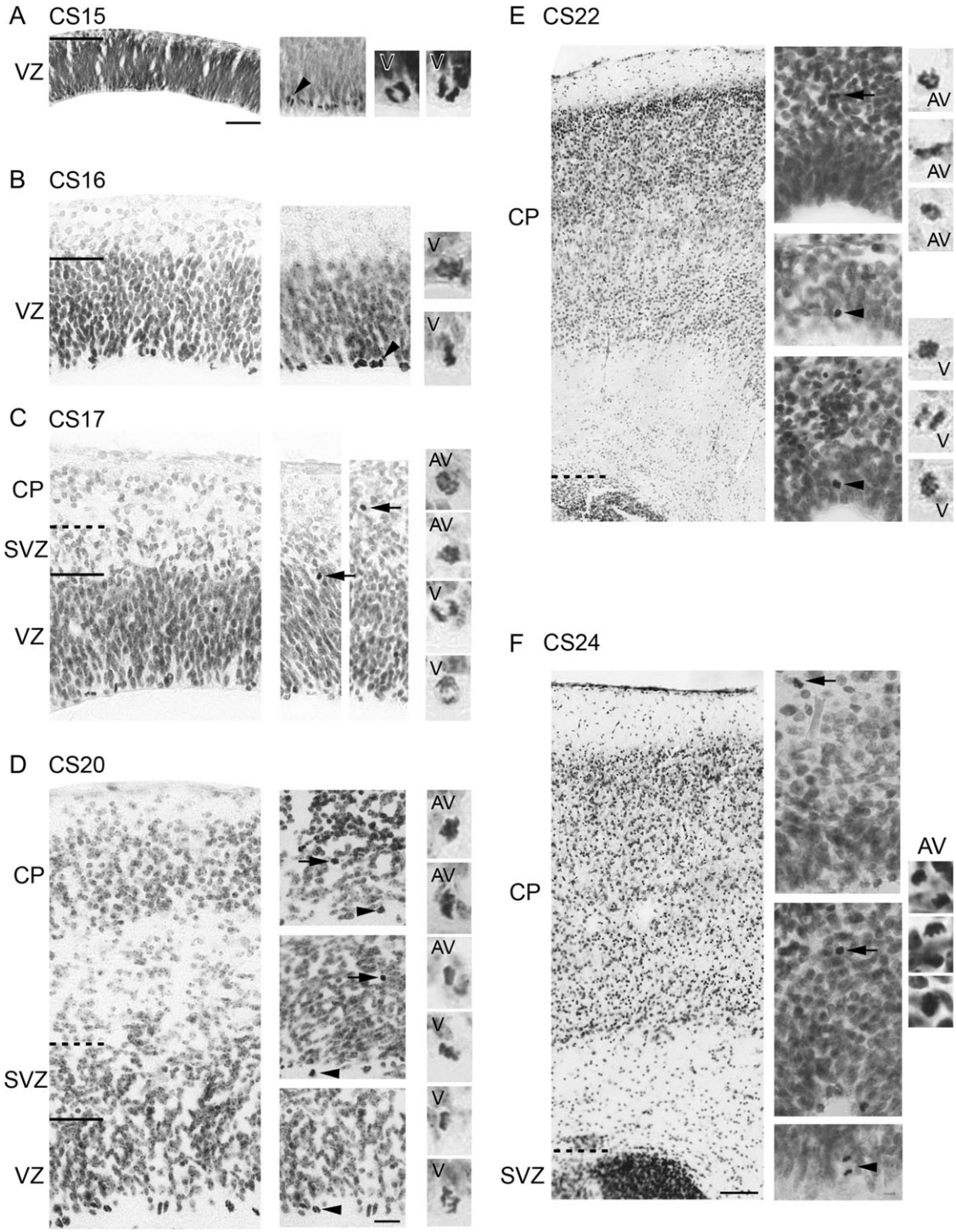

Figure 5. Development of the cortical proliferative zones and cortical plate in *C. perspicillata*. Nissl-stained tissue from bats from CS15 through CS24. (A, B) At CS15 and CS16 the cortex consists of the ventricular and marginal zones and all divisions occur at the surface of the ventricle. (C) At CS17 a thin SVZ becomes apparent and divisions are noted away from the ventricle in the VZ and SVZ. The cortical plate appeared in lateral portions of the cerebral cortex. (D) At CS20 the VZ and SVZ are approximately the same thickness but more divisions occur at the surface of the ventricle. (E) At CS22 the VZ had become very thin and the SVZ was substantially thicker with a notable increase in dividing cells. (F) This trend continued at CS24. The SVZ remained and a few abventricular mitoses were observed. At CS22 and CS24 the cortical plate became thicker as migrating neurons arrived in this structure and began differentiating into recognizable layers. Solid lines delimitate the dorsal border of the VZ. Dashed lines delineate the dorsal border of the SVZ. Arrowheads: ventricular surface mitoses; Arrows: abventricular mitoses. CP: Cortical plate. Calibration bars: In CS15 to CS20: 250 μm; In CS22 and CS2424: 1 mm.

microglial morphology began transitioning from the activated morphology of fetal cells toward the ramified morphology typical in the healthy adult cortex. The CS24 microglia soma were smaller and had more processes that were reduced in thickness (Fig. 11G, H). We have observed the same shift in microglial morphology in the postnatal rat brain (Unpublished observations).

Upon entering the fetal brain microglial cells initially colonize neural proliferative zones and colocalize with neural precursor cells in the rat, monkey, and human cerebral cortex. We have also found that microglia phagocytose neural precursor cells and thereby contribute to regulation of the size of the precursor cell pool, especially in the primate brain (Cunningham et al. 2013). In the bat we did not observe dense colonization of the proliferative zones during neurogenesis as occurs in rat, monkey and human (Cunningham et al. 2013). Nonetheless we found microglial cells contacting neural precursor cells, intercalating between neural precursor cells, and in some cases apparently phagocytosing cells in the proliferative zones (Fig. 11E and F). We co-immunostained sections of CS22 bat cortex with anti-Tbr2 and anti-Iba1 antibodies and found a small number of microglial cells co-localized with the band of Tbr2+ cells in the bat SVZ. These microglia extended processes that intercalated between and contacted neighboring Tbr2+ cells (Fig. 11I and J).

Discussion

While the thickness of the cortical gray matter varies across species, those differences are within an order of magnitude. For example, the thickness of cortical gray matter in mouse at the level of the anterior commissure is ~1.1 mm; in the rat cortex ~1.5 mm thick; in macaque 1.6–2.5 mm; and in human 2.3–3.5 mm (Mikula et al. 2007; Sudheimer et al. 2007). The thickness of the cortical gray matter in *C. perspicillata* is similar to that of mouse at 1.1 mm (Table 1). In contrast, differences in the tangential extent of the cortical sheet vary to a greater degree. For example, the area of the cortical sheet is estimated at 6 cm^2 in rat (Nieuwenhuys et al. 1998), 210 cm^2 in macaque (Van Essen et al. 2012), 2500 cm^2 in human (Peters and Jones 1984) and 6300 in the African elephant (Nieuwenhuys et al. 1998). Thus, while the thickness of mammalian cortical gray matter varies by a factor of 2 or 3 across species, the surface area of the cortical sheet across species can vary by several orders of magnitude.

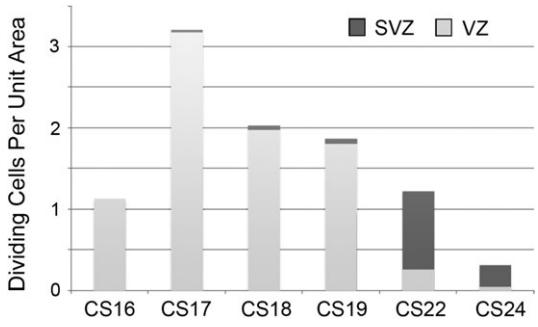

Figure 6. The majority of divisions in the developing bat neocortex occur in the VZ until late stages of neurogenesis at CS22. The number of dividing precursor cells was quantified in 70 micron wide bins that extended from the ventricle across the cortical wall to the pial meninges. Bins were placed in the dorsal cortex of coronal sections at the level of the anterior commissure in *C. perspicillata*. The peak number of divisions per bin occurred at CS17 with over 3 mitoses per bin. The majority of those divisions occurred in the VZ. At CS22 the majority of divisions shifted to the SVZ, but the overall number of mitoses at CS22 was relatively low with just over 1 mitotic figure per bin.

The thickness of the mammalian gray matter is not tightly associated with the degree of gyrencephaly. There are examples of mammals with lissencephalic cortices that have relatively thin and relatively thick gray matter. For example, the mouse cortical gray matter is 1.1 mm thick; marmoset = 1.05 mm; and manatee = 2.8 mm thick. Likewise, there are examples of mammals with highly folded cortices that have gray matter ranging from relatively thin to relatively thick. For example, among gyrencephalic mammals the cortical gray matter ranges from 0.65–1.3 mm thick in dog; 0.95–1.6 mm in cat; 0.9–1.2 mm in ferret; 1.5–2.1 mm in capybara; and 2.3–3.5 mm in human cortex at the crown of cortical gyri (see Table 1).

Understanding how the dynamics of cellular proliferation may contribute to differences in the mammalian cortical sheet will shed light on programs that guide development. In this light, we introduce the bat model of cortical development. There are over 1300 species of bat, they are widespread and naturally inhabit every continent except Antarctica. The length of gestation across bat species varies from 40 days to 6 months, but the longer gestation of some bat species may not necessarily correlate with larger brain size. For example, the normal gestation of *C. perspicillata* is 113–120 days, but the adult brain of *C. perspicillata* in our study weighed 0.588 g, ranking it among the smaller of bat species in terms of brain size. Of further interest for studies of brain development, closely related species of bat have brains of varying size, weight, and cortical folding patterns. Comparative studies across bat species may shed light on developmental mechanisms relevant for understanding mammalian brain development broadly. A key advantage afforded by the relatively long period of organ development in species like *C. perspicillata* is that it allows for greater temporal resolution of specific milestones.

Our data indicate that the neurogenic phase of cortical development in the bat *C. perspicillata* occurs over a period of at least 5 weeks. The cortical neurogenic period is at least 5 times longer than in rat or mouse, yet produces a brain similar in weight, and a neocortex similar in thickness to that of the

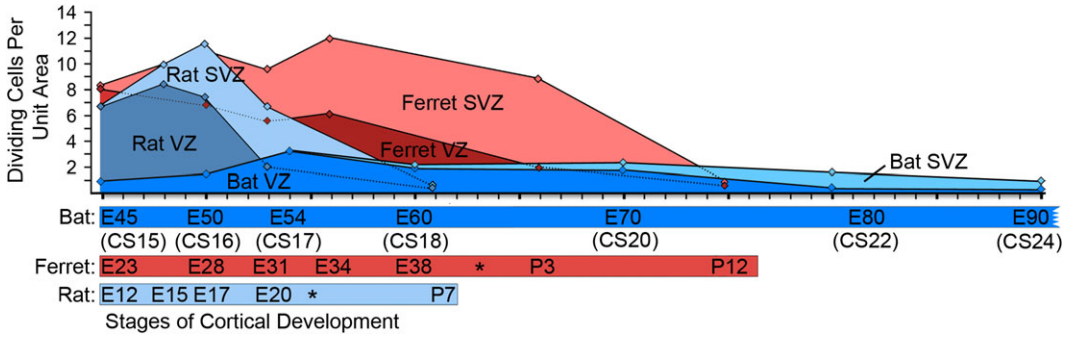

Figure 7. The peak level of cell division in the VZ and SVZ of developing bat neocortex is substantially lower than that in rat or ferret, but the neurogenic phase is considerably longer in bat at approximately 40 days.

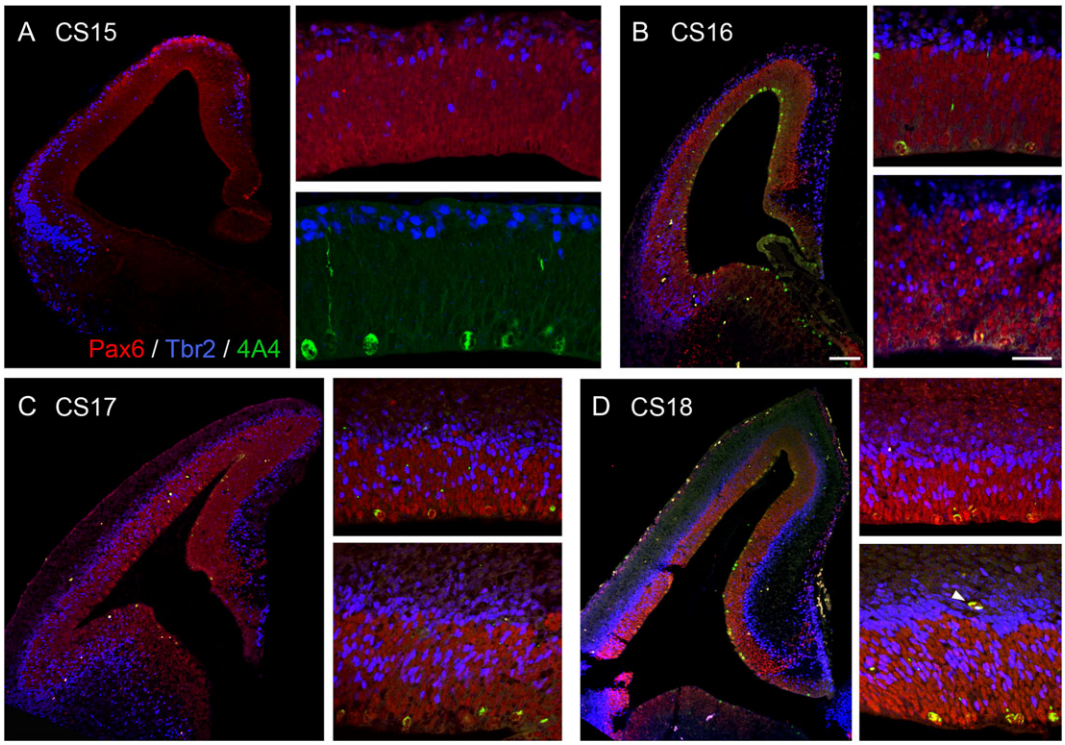

Figure 8. Precursor cells express Pax6 (red) and Tbr2 (blue) during bat neocortical development. (A, B) At CS15 and CS16 Pax6+ precursor cells (red) are present in the VZ and a thin band of Tbr2+ cells (blue) are present in the SVZ. All mitotic cells at CS15 and CS16 (4A4; green) are located at the VZ surface and express Pax6 (red). (C, D) At CS17 and CS18 the Tbr2+ cell band (blue) in the SVZ becomes progressively thicker, but Tbr2+ cells are still dispersed throughout the VZ. Some mitotic cells (4A4; green) in the SVZ express Tbr2 (white arrowhead). Scale bar in B: 100 μm; B inset: 25 μm.

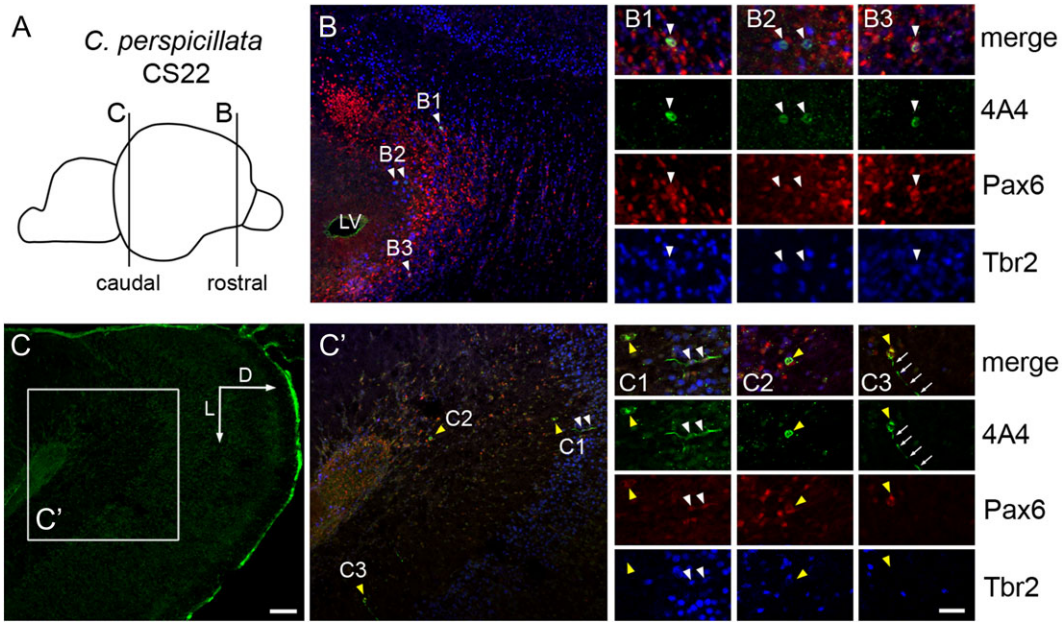

Figure 9. Mitotic Tbr2+ precursor cells are present in the SVZ of CS22 bat cortex. Numerous Tbr2+ cells are present at CS22, particularly in the rostral and caudal poles of the cerebrum. Some mitotic cells in the bat CS22 SVZ (4A4, green) express Pax6 (red) but not Tbr2 (yellow arrowheads). But other mitotic cells express both Pax6 (red) and Tbr2 (blue, white arrowheads). (C3) We also observed 4A4+ cells in the SVZ that possessed apparent pial processes (small white arrows), and that expressed Pax6 but not Tbr2 (yellow arrowhead), suggesting the presence of translocating RG cells in the developing bat cerebral cortex. Scale bar in C: 100 μm; C3: 20 μm.

mouse. Thus, the longer gestation in *C. perspicillata* and in particular the longer neurogenic period, do not correlate with increased brain size or increased cortical folding. Better understanding of how cellular proliferation and cell genesis is regulated in the bat may shed light on signaling pathways that regulate cortical growth in other mammals.

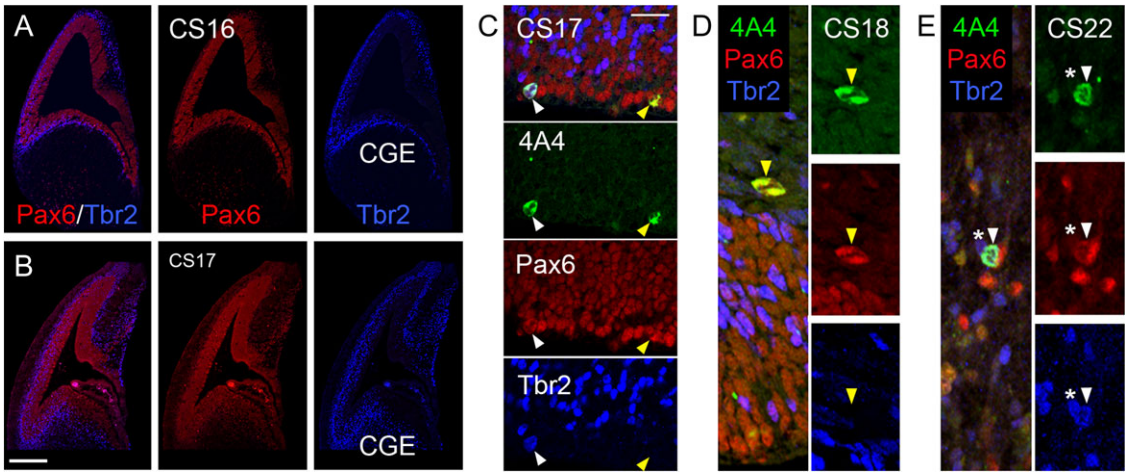

Figure 10. Distribution of Pax6, Tbr2, and dividing precursor cells in *C. perspicillata* cortex. (A, B) Pax6+ precursor cells (red) line the lateral ventricle and Tbr2+ cells (blue) are positioned in the SVZ. Tbr2+ precursor cells were present in the CGE of the CS16 and CS17 bat telencephalon, but were no longer present in the CGE at later stages of development. (C) Mitotic cells (4A4, green) at the surface of the ventricle express Pax6 (red, arrowheads), and some also express Tbr2 (white arrowhead). (D, E) Some abventricular mitoses express Pax6 (red) but not Tbr2 (blue, yellow arrowheads), while other mitoses express both markers (white arrowheads). Mitotic Tbr2+ cells are often adjacent to non-mitotic Tbr2+ cells (asterisk). Scale bar = 1 mm.

Prolonged Neurogenesis in the Bat

We examined the developmental dynamics of the proliferative zones, precursor cell proliferation and cortical plate growth over subsequent stages of cortical development in *C. perspicillata*. We showed that from CS11 through CS15 mitotic precursor cells throughout the cortex divided exclusively at the ventricular surface and that by CS15 Tbr2+ cells were present in the dorsal telencephalon indicating that neural precursor cells were present and that neurogenesis had begun by this stage. The distribution of Tbr2+ cells in the CS15 bat is similar to that at early stages of rat cortical neurogenesis, ~E12/E13 (Noctor et al. 2008). We determined that cortical neurogenesis continued until at least CS23 (E85). Thus, cortical neurogenesis occurs over a period of at least 35 days, ~5 times longer than neurogenesis in mouse or rat. The lengthy neurogenic period in bat does not produce a larger, or gyrencephalic cerebral cortex, but instead a mouse-sized brain, indicating that other key variable(s) must compensate for the lengthy period of cortical histogenesis. Indeed we observed fewer mitoses at the surface of the ventricle, and fewer mitoses away from the ventricle in the SVZ during peak periods of cell genesis in bat cortical development than in rat or ferret. This indicates that fewer cells are dividing at any given timepoint during gestation, and implies that the cell cycle must be substantially longer in this species. A slower rate of cell production would permit the longer neurogenic period in the bat, yet remain within the developmental confines of a mouse-sized cortex.

The length of gestation in *C. perspicillata* averages 120 days, substantially longer than that of similarly sized mammals (Cretekos et al. 2005). But in some cases, *C. perspicillata* gestation may extend beyond 170 days (Rasweiler and Badwaik 1997) as a result of delayed embryonic development. Species from several mammalian orders, including rodents, can exhibit embryonic diapause that occurs after fertilization but before implantation (Mead 1993). In these cases, cell division of the blastocyst is temporarily halted. *C. perspicillata* is in one of five families of bats that may also exhibit prolonged pregnancy resulting from post-implantation delays in development (Orr and Zuk 2014). Seasonal and environmental stressors can initiate developmental pause during gestation. The benefits of developmental delay would include delaying birth during unfavorable conditions as well as timing birth to coincide with sufficient resources to successfully rear young. On the other hand, delayed development may impart substantial costs to the dam that include the increased metabolic demands of carrying an embryo for a longer period and an extended period of maternal immune system suppression (Orr and Zuk 2014). In *C. perspicillata* the pause in gestation usually occurs at the primitive streak stage and can involve reduced or halted cell division (Rasweiler and Badwaik 1997). The capacity to exert this level of control over cellular proliferation during embryo development may also be utilized in the developing forebrain to significantly slow the cell cycle and produce the comparatively long neurogenic period of *C. perspicillata*. This unique feature of bat development therefore offers the potential for gaining insight into factors that regulate cell production, and consequently cortical sheet expansion during development.

Bat Cerebral Cortex Development in Comparison to Other Mammals

We obtained developing brain tissue from wild captured bats spanning Carnegie Stages 11 through 26. For the average gestation length of 113–120 days these stages would represent the developmental period extending from approximately E35 to E90. We found that the CS15 (E46) neocortex of *C. perspicillata* is equivalent to E13 in the rat based on the thickness of the VZ, the location of mitotic cells, and the position of Tbr2+ cells in the superficial portion of the VZ. At E13 in the rat, neurogenesis for preplate neurons occurs (Bayer and Altman 1991) presumably through Tbr2+ precursor cells that are present (Noctor et al. 2008). Our data indicate that the same neurogenic processes are occurring in CS15 *C. perspicillata*. We find that CS16 (E50) is equivalent to E16 in rat based on the appearance of the cortical plate in lateral cortex, and that CS17 is equivalent to E17 in the rat based on the appearance of the SVZ and plentiful abventricular mitoses. Our data suggest that neurogenesis of upper layer neurons continues through CS23 (E85) in the bat, equivalent to the end of layer two neurogenesis in rat (Bayer and Altman 1991), and that cortical tissue from both species are comparable at these 2 stages. Thus, the neurogenic period that occurs within 9 days in the rat encompasses at least 40 days in the bat. For further comparison,

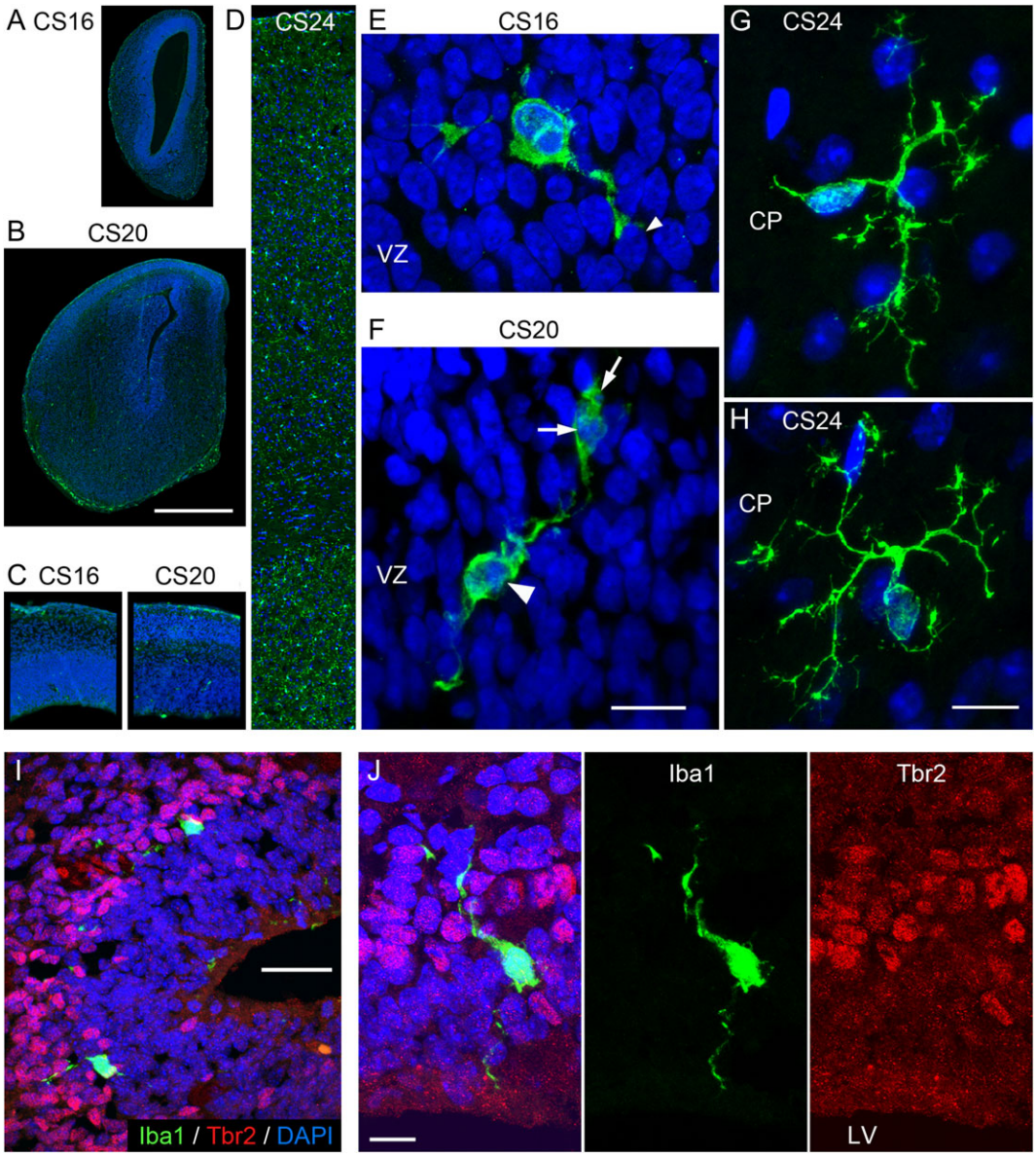

Figure 11. Microglial distribution and morphology in the prenatal bat brain. Sections are immunostained with Iba1 (green), Tbr2 (red), and counterstained with DAPI (blue). Images A, B, and D show CS16, CS20, and S24 bat cortex at the same scale. (*A–C*) Sparse Iba1+ microglial cells (green) are present in the bat neocortex by CS16 through CS20. (*D*) By CS24 microglia they have densely colonized the entire bat neocortex and are distributed evenly across the cortical wall. (*E*) Microglia (green) in the prenatal bat brain proliferative zones exhibit an "activated" morphology with a large soma with a few thick processes. (*F*) A microglial cell in the CS20 VZ (arrowhead) extends a process that envelops another VZ cell (white arrows). (*G*, *H*) By CS24 microglial morphology has begun transitioning from the "activated" morphology of fetal microglia to the more ramified morphology characteristic of healthy adult cortex. Microglia in the CS24 cortex elaborate multiple thinner processes with more ramifications, similar to that seen in a postnatal day 10 rat. (*I*, *J*) Microglia (green) colocalize with Tbr2+ precursor cells (red) in the cortical SVZ. DAPI, blue. Scale bar in B: 500 μm; F, H: 10 μm; J: 5 μm.

the neurogenic period for the much larger and highly folded cortex of rhesus macaque occurs within ~55 days (Rakic 1974). These comparative data are summarized in Table 2.

The length of the cell cycle in macaque (Kornack and Rakic 1998) is longer than that in mouse (Takahashi et al. 1996), and we believe that the cell cycle in bat may be even longer. Another important mechanism that contributes to rapid cortical growth is the 2-step cell amplification (Martínez-Cerdeño et al. 2006), in which Tbr2+ IP cells in the SVZ amplify the output of mitotic RG cells in the VZ. In rats a small proportion of SVZ precursor cells undergo multiple divisions (Hansen et al. 2010), and in some gyrencephalic species it has been shown that Tbr2+ cells undergo symmetric proliferative divisions that further amplify cell production. We show that Tbr2+ cell divisions occur in the bat SVZ (Figure 10), but it is likely that further amplification of the Tbr2+ cell population through symmetric proliferative divisions is limited in the bat.

Sparse Microglial Cell Colonization of the Prenatal Bat Cerebral Cortex

Microglial cells densely colonize the proliferative zones of the prenatal rat and monkey during the latter half of cortical neurogenesis (Cunningham et al. 2013). However, in the bat microglial cell

Table 1 Thickness of adult dorsolateral cortex at the level of the anterior commissure

Species	Scientific name	Cortical Thickness	Source
Mouse	*Mus musculus*	1.11 mm	BrainMaps.org
Rat	*Rattus novegicus*	1.55 mm	BrainMaps.org
Capybara	*Hydrochoerus hydrochaeris*	1.5–2.1 mm	NeuroscienceLibrary.org
Manatee	*Trichechus manatus*	2.8 mm	ManateeBrain.org
Cat	*Felis catus*	0.95–1.6 mm	BrainMaps.org
Dog	*Canis lupus*	1.3 mm	BrainMaps.org
Ferret	*Mustela putorius*	0.9–1.2 mm	Martínez-Cerdeño & Noctor
Marmoset	*Callithrix jacchus*	1.05 mm	NICHD Atlas
Macaque	*Macaca mulatta*	1.6–2.5 mm	BrainMaps.org
Human	*Homo sapiens*	2.3–3.5 mm	MSU Human Brain Atlas
Bat	*Carollia perspicillata*	1.1 mm	Martínez-Cerdeño & Noctor

Table 2 Carnegie stages and gestation age in *C. perspicillata*

Carnegie stage (CS)	Bat approximately day of gestation	Rat equivalent	Macaque equivalent	Key events
Normal gestation length:	113-120 days[a]	22 days	165 days	
CS11	<E40	E11		Neural tube closure
CS12	E40			Ventricular surface divisions
CS14	E44			Ventricular surface divisions
CS15[b]	E46	E13	GD45	Tbr2+ cells present; onset neurogenesis
CS16	E50	E16		Cortical plate appears in lateral cortex
CS17	E54	E17	GD50 (iSVZ)	SVZ forms; abventricular divisions
CS18	E60			Deep cortical layers
CS19	E64	E18		Deep cortical layers
CS20	E70	E19		Layer 4
CS21	E75	E20		Superficial cortical layers
CS22	E80	E21		Superficial cortical layers
CS23[c]	E85	E22	GD104	End of L2 neurogenesis
CS24	E90	P1/3		

[a]Data for *C. perspicillata* are for normal/non-delayed pregnancies. In response to stress in captivity and seasonally in the wild, pregnancies in this species can also be substantially extended beyond 120 days (Rasweiler and Badwaik 1997).
[b]Onset of cortical neurogenesis.
[c]Conclusion of cortical neurogenesis.

distribution in the cortical proliferative zones was comparatively sparse during neurogenic stages. The number of microglia in the bat cortex during prenatal neurogenesis was less than that seen at comparative developmental stages in the rat (Cunningham et al. 2013). There were a small number of microglial cells that co-localized among Tbr2+ cells in the bat proliferative zone. Despite the small population of microglia colonizing bat neocortex, we observed examples of cellular phagocytosis in the bat cortical proliferative zones (Fig. 11F), as occurs in rat and macaque (Cunningham et al. 2013). Our previous findings indicate that in the fetal rat brain, and especially in the fetal macaque brain, one function of microglial cells is to regulate precursor cell number (Cunningham et al. 2013). The relatively low number of microglia in the proliferative zones of the prenatal bat cortex may allow sufficient cell production given the comparatively slow rate of precursor cell division. Phagocytosis of precursor cells is much more prominent in the primate brain, which may be associated with the substantially larger precursor cell population in the developing macaque brain.

Tbr2 is Expressed in the Bat CGE

Pax6 and Tbr2 expression in *C. perspicillata* largely mirrored that previously shown in the developing brain of other mammals. One interesting aspect of cortical development in the bat was marked Tbr2 expression in the CGE. Previous work in rodent indicates that Tbr2 expression is absent in the ganglionic eminences, and that precursor cells in the ganglionic eminences do not generate neurons via the Tbr2+ lineage. Evidence supporting this concept includes: lack of Tbr2 expression in the GE (Englund et al. 2005), lack of Tbr2 lineage reporter expression by cortical interneurons generated in the ganglionic eminences (Vasistha et al. 2015; Mihalas et al. 2016), and that precursor cells in the CGE do not produce Tbr1-expressing projection neurons (Nery et al. 2002). Similar findings have been reported for human and nonhuman primate CGE (Ma et al. 2013). However, we found strong Trb2 expression in the bat CGE at CS16 and CS17 (Fig. 10), stages that correspond to approximately E15-E17 in the rat. We did not observe Tbr2+ cells in the CGE of E17 rat. Tbr2 expression in the bat CGE may represent the generation of a unique set of projection neurons that are not widely present in other mammals. Tbr2 expression has been reported in the region of the developing chick forebrain that corresponds to the CGE (Bulfone et al. 1999), so there is precedent for Tbr2+ cells in ventral proliferative structures of some vertebrate brains. It is possible that some cortical areas in the bat exhibit unique cellular composition in comparison to other mammals that are related to specialized behaviors. On the other hand,

Tbr2 expression in the bat CGE could simply reflect the production of projection neurons destined for the occipital cortex in the caudal pole of the telencephalon. It is also possible that a brief period of Tbr2 expression occurs in the CGE of rodents that have a compressed neurogenic period, but that this expression is more easily identified in species like the bat that have a substantially longer neurogenic period. Consistent with this idea, by CS18 Tbr2+ cells were no longer present in the CGE, and from this stage on Tbr2 expression in the bat matched that described for other mammals. Overall, the temporal dynamics of transcription factor expression in the bat matched that described in rodent models.

Summary

The short-tailed fruit bat offers unique advantages in comparison to other commonly used model species, including: (1) a longer neurogenic period that can yield greater temporal resolution for specific stages of neuro- and gliogenesis; (2) an apparently slow cell cycle that presents opportunities for genetic screening to identify novel molecular targets that regulate the cell cycle; and (3) bats are known to be natural reservoirs for many dangerous pathogens. A representative of this group that is easy to maintain in a research setting may provide a valuable model for understanding how the immune system responds to such organisms and how the maternal immune system impacts the development of fetal organs under pathological conditions.

Funding

This work was supported by NIH grant MH094681 to V.M.C., MH101188 to S.C.N., the MIND Institute (IDDRC; U54 HD079125), and the Shriners Hospitals.

Notes

Mcollected either from the wild on the West Indian island of Trinidad (Rasweiler and Badwaik, 2005a) or born, raised, and then bred in a laboratory colony. The wild-caught specimens were collected and exported with the permission of the Wildlife Section, Forestry Division of the Ministry of Agriculture, Land and Marine Re-sources of the Republic of Trinidad and Tobago. The colony was main-at the Weill Medical College of Cornell University in accordance with the "Principles of Laboratory Animal Care" (NIH publication no. 86-23). *Conflict of Interest*: None declared.

References

Altman J, Bayer SA. 1995. Atlas of prenatal rat brain development. Boca Raton, FL: CRC Press.

Badwaik NK, Rasweiler JJ IV. 2001. Altered trophoblastic differentiation and increased trophoblastic invasiveness during delayed development in the short-tailed fruit bat, Carollia perspicillata. Placenta. 22:124–144.

Baron G, Stephan H, Frahm HD. 1996. Macromorphology, brain structures, tables and atlases. Basel: Birkhauser Verlag.

Bayer SA, Altman J. 1991. Neocortical development. New York: Raven Press.

Bulfone A, Martinez S, Marigo V, Campanella M, Basile A, Quaderi N, Gattuso C, Rubenstein JL, Ballabio A. 1999. Expression pattern of the Tbr2 (Eomesodermin) gene during mouse and chick brain development. Mech Dev. 84:133–138.

Cretekos CJ, Weatherbee SD, Chen CH, Badwaik NK, Niswander L, Behringer RR, Rasweiler JJ IV. 2005. Embryonic staging system for the short-tailed fruit bat, Carollia perspicillata, a model organism for the mammalian order Chiroptera, based upon timed pregnancies in captive-bred animals. Dev Dyn. 233:721–738.

Cunningham CL, Martinez-Cerdeno V, Noctor SC. 2013. Microglia regulate the number of neural precursor cells in the developing cerebral cortex. J Neurosci. 33:4216–4233.

deAzevedo LC, Fallet C, Moura-Neto V, Daumas-Duport C, Hedin-Pereira C, Lent R. 2003. Cortical radial glial cells in human fetuses: depth-correlated transformation into astrocytes. J Neurobiol. 55:288–298.

Englund C, Fink A, Lau C, Pham D, Daza RA, Bulfone A, Kowalczyk T, Hevner RF. 2005. Pax6, Tbr2, and Tbr1 are expressed sequentially by radial glia, intermediate progenitor cells, and postmitotic neurons in developing neocortex. J Neurosci. 25:247–251.

Fietz SA, Kelava I, Vogt J, Wilsch-Brauninger M, Stenzel D, Fish JL, Corbeil D, Riehn A, Distler W, Nitsch R, et al. 2010. OSVZ progenitors of human and ferret neocortex are epithelial-like and expand by integrin signaling. Nat Neurosci. 13:690–699.

Gotz M, Stoykova A, Gruss P. 1998. Pax6 controls radial glia differentiation in the cerebral cortex. Neuron. 21:1031–1044.

Graham GL, Reid FA. 2001. Bats of the world. New York, NY: St. Martin's Press.

Hamilton A. 1901. The division of differentiated cells in the central nervous system of the white rat. J Comp Neurol. 11: 297–322.

Hansen DV, Lui JH, Parker PR, Kriegstein AR. 2010. Neurogenic radial glia in the outer subventricular zone of human neocortex. Nature. 464:554–561.

Ibanez Rodriguez MP, Noctor SC, Munoz EM. 2016. Cellular basis of pineal gland development: emerging role of microglia as phenotype regulator. PLoS ONE. 11:e0167063.

Kornack DR, Rakic P. 1998. Changes in cell-cycle kinetics during the development and evolution of primate neocortex. Proc Natl Acad Sci U S A. 95:1242–1246.

Ma T, Wang C, Wang L, Zhou X, Tian M, Zhang Q, Zhang Y, Li J, Liu Z, Cai Y, et al. 2013. Subcortical origins of human and monkey neocortical interneurons. Nat Neurosci. 16: 1588–1597.

Martinez-Cerdeno V, Cunningham CL, Camacho J, Antczak JL, Prakash AN, Cziep ME, Walker AI, Noctor SC. 2012. Comparative analysis of the subventricular zone in rat, ferret and macaque: evidence for an outer subventricular zone in rodents. PLoS ONE. 7:e30178.

Martinez-Cerdeno V, Cunningham CL, Camacho J, Keiter JA, Ariza J, Lovern M, Noctor SC. 2016. Evolutionary origin of Tbr2-expressing precursor cells and the subventricular zone in the developing cortex. J Comp Neurol. 524:433–447.

Martinez-Cerdeno V, Noctor SC. 2016. Cortical evolution 2015: discussion of neural progenitor cell nomenclature. J Comp Neurol. 524:704–709.

Martínez-Cerdeño V, Noctor SC, Kriegstein AR. 2006. The role of intermediate progenitor cells in the evolutionary expansion of the cerebral cortex. Cereb Cortex. 16:152–161.

Mead RA. 1993. Embryonic diapause in vertebrates. J Exp Zool. 266:629–641.

Mihalas AB, Elsen GE, Bedogni F, Daza RA, Ramos-Laguna KA, Arnold SJ, Hevner RF. 2016. Intermediate progenitor cohorts differentially generate cortical layers and require Tbr2 for timely acquisition of neuronal subtype identity. Cell Rep. 16: 92–105.

Mikula S, Trotts I, Stone J, Jones EG 2007. BrainMaps: An Interactive Multiresolution Brain Atlas. In.

Miyata T, Kawaguchi A, Saito K, Kawano M, Muto T, Ogawa M. 2004. Asymmetric production of surface-dividing and non-surface-dividing cortical progenitor cells. Development. 131: 3133–3145.

Nery MF, Gonzalez DJ, Hoffmann FG, Opazo JC. 2012. Resolution of the laurasiatherian phylogeny: evidence from genomic data. Mol Phylogenet Evol. 64:685–689.

Nery S, Fishell G, Corbin JG. 2002. The caudal ganglionic eminence is a source of distinct cortical and subcortical cell populations. Nat Neurosci. 5:1279–1287.

Nieuwenhuys R, ten Donkelaar HJ, Nicholson C. 1998. The central nervous system of vertebrates. Berlin: Springer.

Noctor SC, Flint AC, Weissman TA, Dammerman RS, Kriegstein AR. 2001. Neurons derived from radial glial cells establish radial units in neocortex. Nature. 409:714–720.

Noctor SC, Martínez-Cerdeño V, Ivic L, Kriegstein AR. 2004. Cortical neurons arise in symmetric and asymmetric division zones and migrate through specific phases. Nat Neurosci. 7:136–144.

Noctor SC, Martinez-Cerdeño V, Kriegstein AR. 2008. Distinct behaviors of neural stem and progenitor cells underlie cortical neurogenesis. J Comp Neurol. 508:28–44.

Orr TJ, Zuk M. 2014. Reproductive delays in mammals: an unexplored avenue for post-copulatory sexual selection. Biol Rev Camb Philos Soc. 89:889–912.

Peters A, Jones EG. 1984. Cerebral Cortex. In: Jones EG, Peters A, editors. Cerebral Cortex. New York: Plenum Press. p. 107–121.

Rakic P. 1974. Neurons in rhesus monkey visual cortex: systematic relation between time of origin and eventual disposition. Science. 183:425–427.

Rasweiler JJ IV, Badwaik NK. 1997. Delayed development in the short-tailed fruit bat, Carollia perspicillata. J Reprod Fertil. 109:7–20.

Rasweiler JJ IV, Cretekos CJ, Behringer RR. 2009. The short-tailed fruit bat Carollia perspicillata: a model for studies in reproduction and development. Cold Spring Harb protoc. 2009: pdb emo118.

Reillo I, de Juan Romero C, Garcia-Cabezas MA, Borrell V. 2011. A role for intermediate radial glia in the tangential expansion of the mammalian cerebral cortex. Cereb Cortex. 21:1674–1694.

Sauer FC. 1935. Mitosis in the neural tube. J Comp Neurol. 62: 377–405.

Schmechel DE, Rakic P. 1979. A Golgi study of radial glial cells in developing monkey telencephalon: morphogenesis and transformation into astrocytes. Anat Embryol. 156:115–152.

Seymour RM, Berry M. 1975. Scanning and transmission electron microscope studies of interkinetic nuclear migration in the cerebral vesicles of the rat. J Comp Neurol. 160:105–125.

Smart IH. 1973. Proliferative characteristics of the ependymal layer during the early development of the mouse neocortex: a pilot study based on recording the number, location and plane of cleavage of mitotic figures. J Anat. 116:67–91.

Smart IH, Dehay C, Giroud P, Berland M, Kennedy H. 2002. Unique morphological features of the proliferative zones and postmitotic compartments of the neural epithelium giving rise to striate and extrastriate cortex in the monkey. Cereb Cortex. 12:37–53.

Springer MS. 2013. Phylogenetics: bats united, microbats divided. Curr Biol. 23:R999–R1001.

Sudheimer KD, Winn BM, Kerndt GM, Shoaps JM, Davis KK, Fobbs AJ, Johnson JI 2007. Michigan State University Brain Biodiversity Bank: the Human Brain Atlas. In.

Takahashi T, Nowakowski RS, Caviness V Jr.. 1993. Cell cycle parameters and patterns of nuclear movement in the neocortical proliferative zone of the fetal mouse. J Neurosci. 13: 820–833.

Takahashi T, Nowakowski RS, Caviness VS. 1996. The leaving or Q fraction of the murine cerebral proliferative epithelium: a general model of neocortical neuronogenesis. J Neurosci. 16:6183–6196.

Van Essen DC, Glasser MF, Dierker DL, Harwell J. 2012. Cortical parcellations of the macaque monkey analyzed on surface-based atlases. Cereb Cortex. 22:2227–2240.

Vasistha NA, Garcia-Moreno F, Arora S, Cheung AF, Arnold SJ, Robertson EJ, Molnar Z. 2015. Cortical and clonal contribution of Tbr2 expressing progenitors in the developing mouse brain. Cereb Cortex. 25:3290–3302.

Voigt T. 1989. Development of glial cells in the cerebral wall of ferrets: direct tracing of their transformation from radial glia into astrocytes. J Comp Neurol. 289:74–88.